Volume 14
Number 45
7 December 2023
Pages 12801–13266

Chemical Science

rsc.li/chemical-science

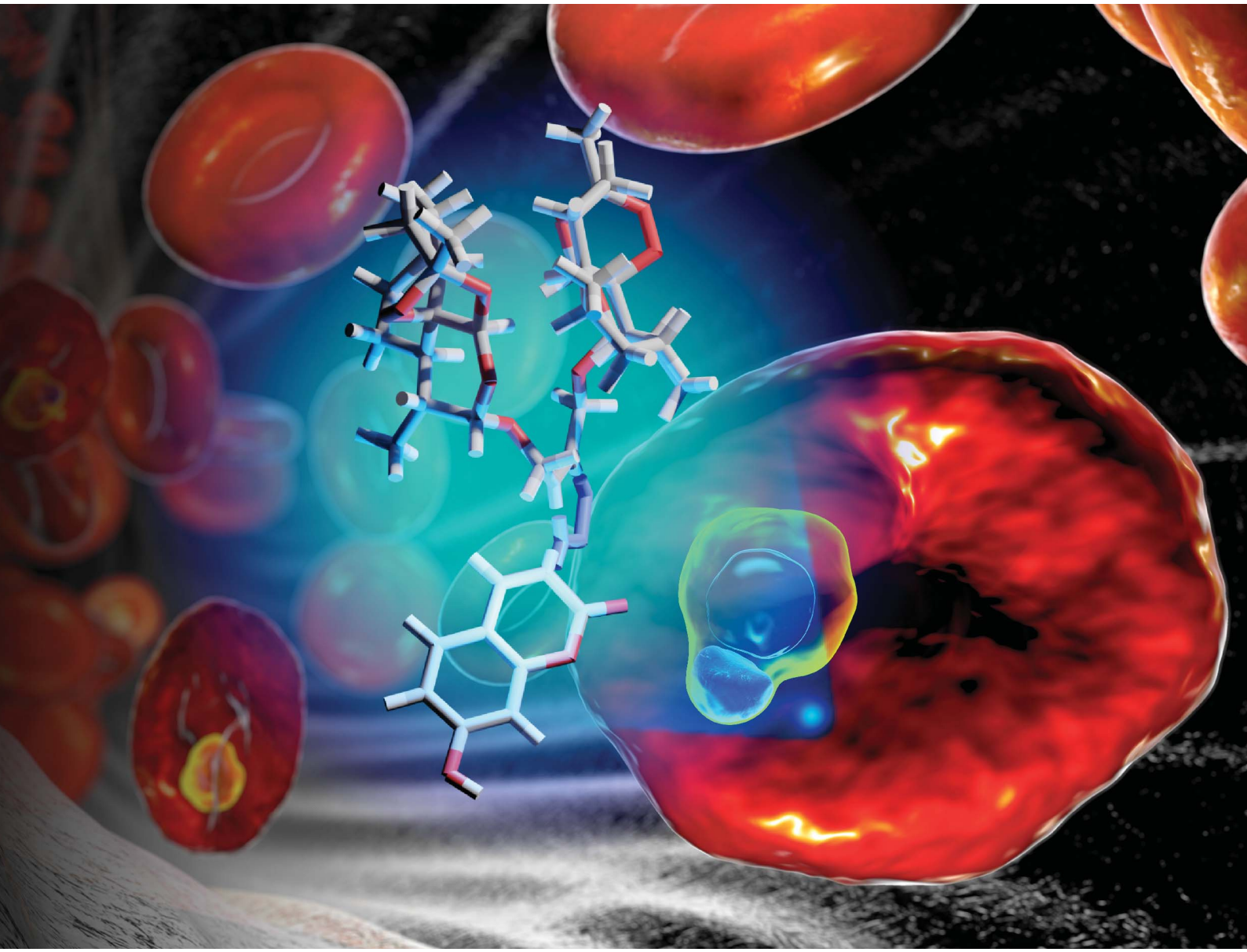

ISSN 2041-6539

ROYAL SOCIETY OF CHEMISTRY

EDGE ARTICLE

Diogo R. M. Moreira, Barbara Kappes, Svetlana B. Tsogoeva *et al.*
Autofluorescent antimalarials by hybridization of artemisinin and coumarin: *in vitro/in vivo* studies and live-cell imaging

Chemical Science

ROYAL SOCIETY OF CHEMISTRY

EDGE ARTICLE

View Article Online
View Journal | View Issue

Cite this: *Chem. Sci.*, 2023, **14**, 12941

All publication charges for this article have been paid for by the Royal Society of Chemistry

Autofluorescent antimalarials by hybridization of artemisinin and coumarin: *in vitro*/*in vivo* studies and live-cell imaging†

Lars Herrmann,[a] Maria Leidenberger,[b] Adrielle Sacramento de Morais,[c] Christina Mai,[a] Aysun Çapci,[a] Mariana da Cruz Borges Silva,[c] Fabian Plass,[de] Axel Kahnt,[de] Diogo R. M. Moreira,*[c] Barbara Kappes*[b] and Svetlana B. Tsogoeva*[a]

Received 17th July 2023
Accepted 22nd October 2023

DOI: 10.1039/d3sc03661h

rsc.li/chemical-science

Malaria is one of our planet's most widespread and deadliest diseases, and there is an ever-consistent need for new and improved pharmaceuticals. Natural products have been an essential source of hit and lead compounds for drug discovery. Antimalarial drug artemisinin (ART), a highly effective natural product, is an enantiopure sesquiterpene lactone and occurs in *Artemisia annua* L. The development of improved antimalarial drugs, which are highly potent and at the same time inherently fluorescent is particularly favorable and highly desirable since they can be used for live-cell imaging, avoiding the requirement of the drug's linkage to an external fluorescent label. Herein, we present the first antimalarial autofluorescent artemisinin-coumarin hybrids with high fluorescence quantum yields of up to 0.94 and exhibiting excellent activity *in vitro* against CQ-resistant and multidrug-resistant *P. falciparum* strains (IC_{50} (Dd2) down to 0.5 nM; IC_{50} (K1) down to 0.3 nM) compared to reference drugs CQ (IC_{50} (Dd2) 165.3 nM; IC_{50} (K1) 302.8 nM) and artemisinin (IC_{50} (Dd2) 11.3 nM; IC_{50} (K1) 5.4 nM). Furthermore, a clear correlation between *in vitro* potency and *in vivo* efficacy of antimalarial autofluorescent hybrids was demonstrated. Moreover, deliberately designed autofluorescent artemisinin-coumarin hybrids, were not only able to overcome drug resistance, they were also of high value in investigating their mode of action *via* time-dependent imaging resolution in living *P. falciparum*-infected red blood cells.

Introduction

Nature is an excellent source of drugs or their precursors.[1] Antimalarial drug artemisinin (Fig. 1a) is a prominent natural product. It is an enantiomerically pure sesquiterpene lactone found in *Artemisia annua* L. Its discoverer Youyou Tu was awarded the 2015 Nobel Prize in Physiology or Medicine.[2,3] Artemisinin and its derivatives are of great interest for their vast range of biological properties.[4,5] Target identification experiments have recently been performed, and putative inhibitory mechanisms of artemisinin-related compounds have been studied.[6–8] Notably, one of the most powerful tools to address the mode of action of bioactive compounds is an investigation *via* fluorescence-based techniques.[9,10] A fluorescent non-drug label is commonly introduced into a drug molecule to make it suitable for live-cell fluorescence tracking.[11,12] In the past, this approach was also applied to artemisinins.[13–16] Though fluorescent labeling enables localization imaging, the concept has significant drawbacks. The drug's polarity, solubility, cellular uptake, biological activity, and mode of action can significantly alter as the pristine drugs are heavily altered and enlarged.[17,18] One possible pathway to circumnavigate drawbacks accompanied by fluorescent labeling is the design and application of inherently fluorescent bioactive hybrids, which are potent drug compounds and fluorophores at the same time.[17,19] The efficacy of hybrid drugs and their potential to overcome even drug resistance has been widely proven.[20–29] To our knowledge, no examples of inherently fluorescent antimalarial hybrid drugs have been reported so far. The aim of this work is, therefore, to combine two desired features in one artemisinin-based antimalarial hybrid drug: (i) high *in vitro*/*in vivo* activity and (ii) high

[a]*Organic Chemistry Chair I and Interdisciplinary Center for Molecular Materials (ICMM), Friedrich-Alexander-Universität Erlangen-Nürnberg, Nikolaus-Fiebiger-Straße 10, 91054 Erlangen, Germany. E-mail: svetlana.tsogoeva@fau.de*

[b]*Institute of Medical Biotechnology, Friedrich-Alexander-Universität Erlangen-Nürnberg, Paul-Gordon-Straße 3, 91052 Erlangen, Germany. E-mail: barbara.kappes@fau.de*

[c]*Instituto Gonçalo Moniz, Fundação Oswaldo Cruz, Salvador 40296-710, Brazil. E-mail: diogo.magalhaes@fiocruz.br*

[d]*Leibniz Institute of Surface Engineering (IOM), Permoserstrasse 15, 04318 Leipzig, Germany*

[e]*Physical Chemistry Chair I, Friedrich-Alexander-Universität Erlangen-Nürnberg, Egerlandstrasse 3, 91058 Erlangen, Germany*

† Electronic supplementary information (ESI) available: Synthetic procedures, fluorescence and NMR spectra of the hybrid compounds, additional biological data and explanations. See DOI: https://doi.org/10.1039/d3sc03661h

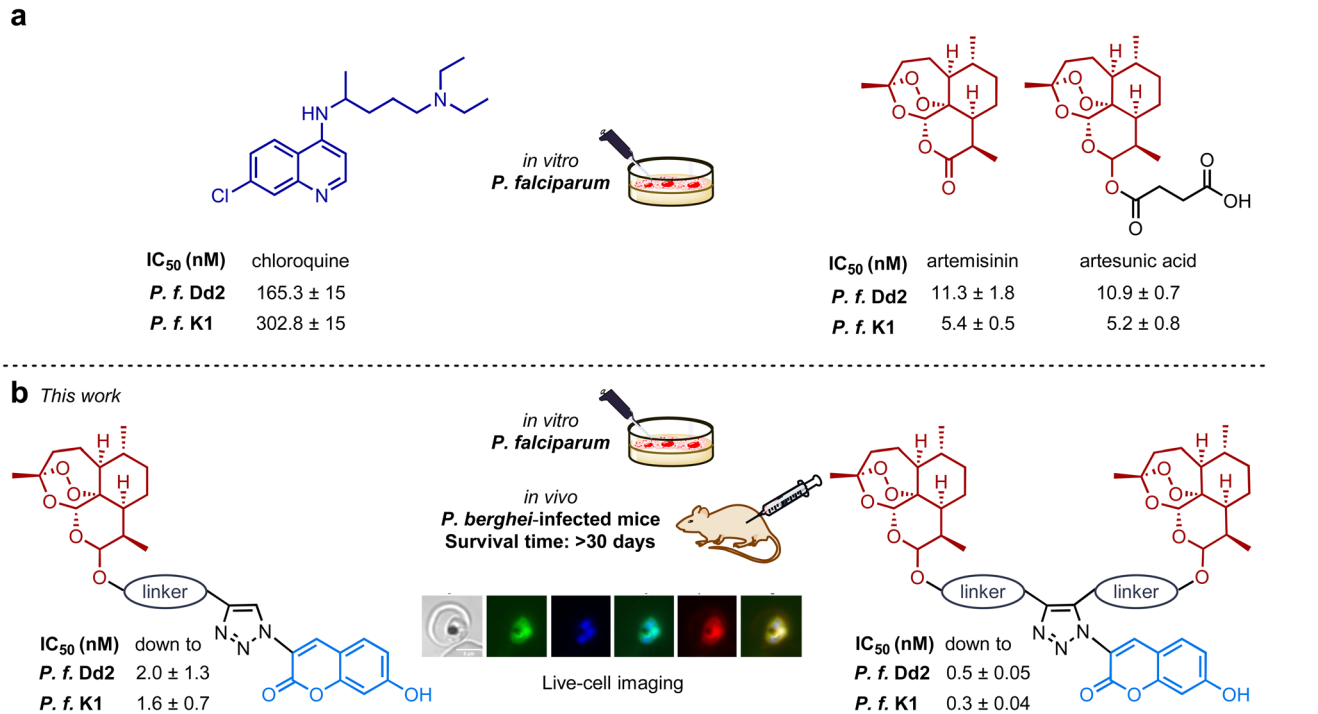

Fig. 1 (a) Structures of established antimalarials chloroquine, artemisinin and artesunic acid and their *in vitro* activity against CQ-resistant and multidrug-resistant *P. falciparum* strains Dd2 and K1. (b) The first systematic comparison of antimalarial activities of differently linked monomeric and dimeric artemisinin-based hybrid model drugs using *in vitro*, *in vivo* and live-cell bioimaging methods.

intrinsic fluorescence. To design fluorescent artemisinin-based antimalarial hybrids, an additional bioactive species is required to gain improved antiplasmodial activity and to enable autofluorescence. We selected bioactive coumarins as prominent and suitable pharmacophores. While few examples of anticancer artemisinin-coumarin hybrids are known,[30–32] no examples of antimalarial artemisinin-coumarin hybrid compounds and their *in vitro*/*in vivo* analyses and mode of action studies have been reported to date. Coumarin derivatives *e.g.*, scopoletin, showing antimalarial properties, and other derivates naturally occur with artemisinin in *Artemisia annua* L.[33–37] In addition to their antimalarial properties, coumarin derivatives exhibit activities against a broad scope of pathogens[38–41] and are highly suitable for synthesizing intrinsically fluorescent hybrids since they can be tuned to be strongly fluorescent by binding to a triazole subunit.[42,43]

Artemisinin-derived fluorescence tracers for localization imaging, especially in red blood cells infected with living parasites of *P. falciparum*, are rare[44] and to the best of our knowledge, no time-dependent studies investigating possible changes in subcellular localization of such compounds in dependence on the incubation time have been performed. Herein, we present the first antimalarial autofluorescent artemisinin-coumarin hybrids and their biological *in vitro* studies against chloroquine-sensitive 3D7 and chloroquine-/multidrug-resistant Dd2 and K1 parasite strains of *P. falciparum*, and *in vivo* studies in *P. berghei*-infected mice (Fig. 1b). The use of triazoles as subunits in hybrid drugs is beneficial apart from their ability to induce fluorescence, as these heterocyclic subunits can easily be formed *via* click chemistry.[45,46]

We used the strong autofluorescence of new hybrid drugs (fluorescence quantum yields up to 0.94) to investigate the subcellular localization and to achieve a live-cell *P. falciparum* parasite imaging under unprecedented conditions that mimic treatment with artemisinin (ART) in humans. Next, the stability of the implemented linkers between the triazole and artemisinin subunit (non-cleavable (ether) *vs.* cleavable (ester) linkers) has been firmly taken into consideration as it is broadly accepted that artemisinins are relatively short-lived prodrugs primarily metabolized *via* heme-mediated degradation[47,48] and the linker significantly affects the elimination half-lives.[49,50]

Results

Synthesis of artemisinin-coumarin hybrid compounds

In the past, our and other groups showed the high potential of dimeric artemisinin-based hybrids exhibiting strongly improved activities against malaria and other pathogens.[8,51–55] In this study, we first intended to understand the differences in efficacy of dimeric *vs.* monomeric artemisinin-based hybrids concerning the applied linker moieties (cleavable *vs.* non-cleavable). For those studies, the monomeric artemisinin-coumarin hybrids **1** and **2** were synthesized *via* copper(I)-catalyzed azide-alkyne cycloaddition (CuAAC) click reactions (Scheme 1a). The monomeric artemisinin-alkyne precursors were obtained in good yields (**7**: 74%/**9**: 94%) *via* two diverse straightforward one-step procedures,[29,56] whereas the coumarin azide **11** was commercially available (Scheme 1).

Hybrid **1** was prepared in 45% yield *via* CuAAC between alkyne **7** and the coumarin azide **11** using $CuSO_4$ and sodium

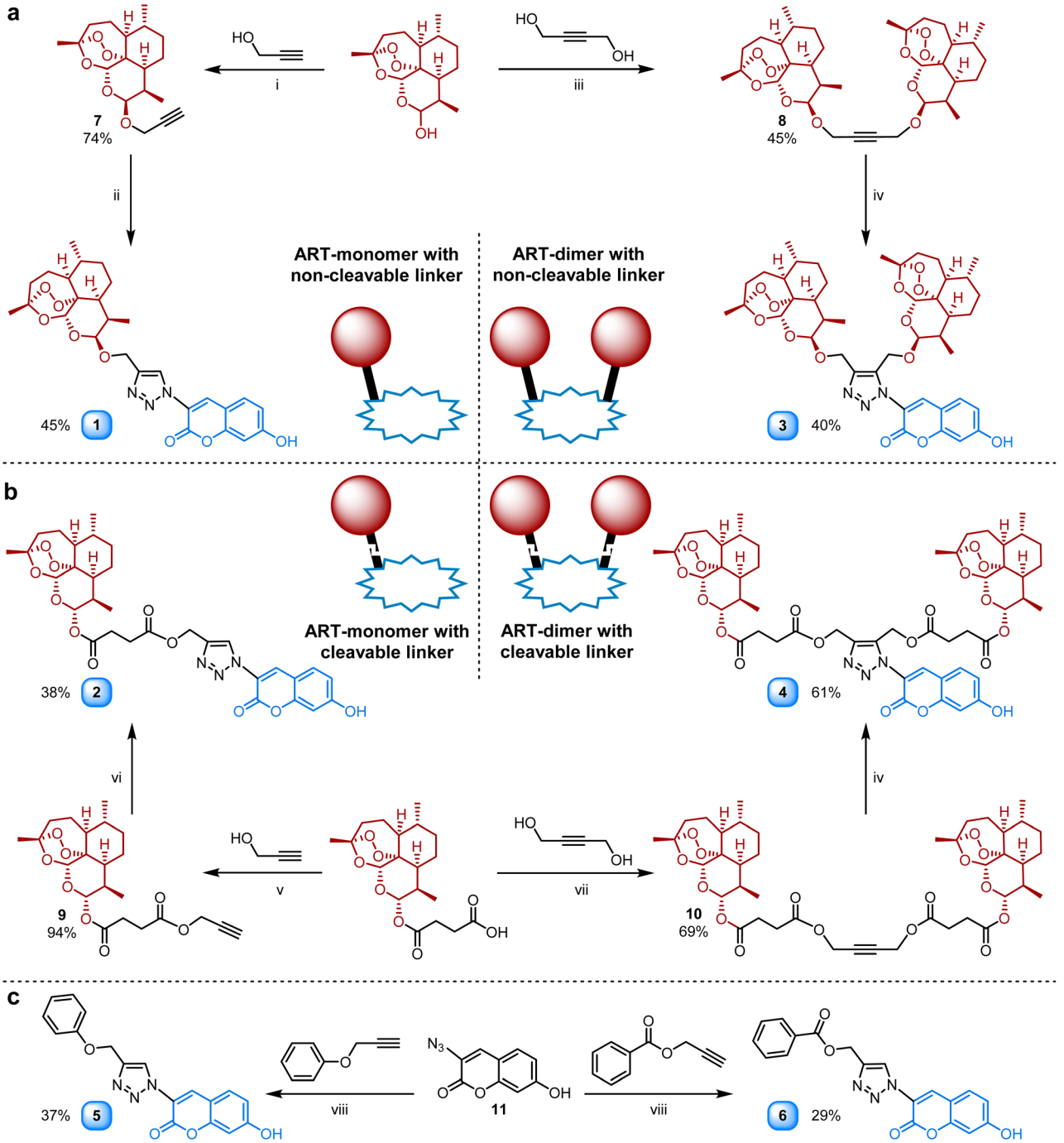

Scheme 1 (a) Synthesis of non-cleavable linker-containing artemisinin-coumarin hybrids **1** and **3** derived from DHA. (b) Synthesis of cleavable linker-containing artemisinin-coumarin hybrids **2** and **4** derived from artesunic acid. (c) Synthesis of reference coumarin-triazoles **5** and **6** bearing no artemisinin unit. Reagents and conditions: (i) $H_3PW_{12}O_{40}\cdot H_2O$ (10 mol%), DCM, r.t., 6 h; (ii) coumarin-azide **11**, $CuSO_4\cdot 5H_2O$ (10 mol%), sodium ascorbate (20 mol%), $CH_2Cl_2 : H_2O$ (1 : 1), r.t., o/n; (iii) $BF_3\cdot Et_2O$, Et_2O, N_2, r.t., 24 h; (iv) coumarin-azide **11**, [Cp*Ru(cod)Cl] (2 mol%), DMF, Ar., r.t., 24 h; (v) EDCI, DMAP, DCM, N_2, 0 °C to r.t., o/n.; (vi) coumarin-azide **11**, $CuSO_4\cdot 5H_2O$ (20 mol%), sodium ascorbate (40 mol%), DMF, Ar., r.t., 1 h; (vii) EDCI, DMAP, DCM/acetonitrile (6/1), 0 °C to r.t., o/n.; (viii) $CuSO_4\cdot 5H_2O$ (20 mol%), sodium ascorbate (40 mol%), DMF, Ar., r.t., 1 h.

ascorbate in a diphasic solvent system (DCM:H_2O). On the other hand, a monophasic CuAAC reaction with $CuSO_4$ and ascorbic acid in DMF between the artesunic acid-derived alkyne **9** and coumarin azide **11** was performed to gain hybrid **2** in 38% yield. Two dimeric-artemisinin precursors **8** and **10** with an internal alkyne were prepared to synthesize hybrids **3** and **4** (Scheme 1b) bearing two artemisinin units. The DHA (dihydroartemisinin) based dimeric alkyne precursor **8** was synthesized starting from a 1 : 1 mixture of C-10α-to C-10β-DHA *via* a newly developed etherification procedure using $BF_3\cdot EtO_2$ (Scheme 1a). The

product **8** with two C-10β-DHA units was isolated in a fair yield of 45% and the C-10β configuration was verified with ^{1}H-NMR.[57] Alkyne **10** derived from artesunic acid was obtained *via* a literature-known procedure in 69% yield (Scheme 1b).[58] Since internal alkynes have to be activated for the cycloaddition towards hybrids **3** and **4** to take place, a Ru(II) based catalyst ([Cp*Ru(cod)Cl], 2 mol%) was applied instead of the copper-based systems used for the synthesis of hybrids **1** and **2**. The hybrid compounds **3** and **4** were synthesized with an identical procedure in anhydrous DMF under argon and isolated in fair yields (**3**: 40%/**4**: 61%). The reference compounds **5** and **6** (Scheme 1c) bearing no artemisinin unit were prepared to have a comparison to the artemisinin-derived hybrids **1–4**. The corresponding commercially available ether-/ester-bridged alkynes were coupled with coumarin azide **11** *via* CuAAC in DMF to obtain both triazole-coumarins (**5**: 37% yield/**6**: 29% yield, Scheme 1c).

Fluorescence properties of the compounds

All compounds **1–6** bear a 7-hydroxo-cumarine fluorophore covalently attached over a triazole moiety which dominates the optical properties of the hybrids. The observed UV-vis absorption and fluorescence spectra (see Fig. S6–11†), align with previous results for covalently functionalized 7-hydroxy-cumarine derivatives.[59–61] Essentially and in line with previous literature reports[59–61] for functionalized 7-hydroxy-cumarine derivatives, all investigated compounds show a red shift of around 15 nm in the long wavelength absorption maximum (see Table 1) compared to pristine 7-hydroxy-cumarine, which exhibits a long-wavelength absorption maximum around 330 nm.[62,63] This red shift of the absorption goes hand in hand with a red shift of the fluorescence maximum observed for compounds **1–6** (between 410 and 435 nm – *cf.* Table 1) in respect to pristine 7-hydroxy-cumarine, which is reported to exhibit a fluorescence maximum around 380 nm in ethanol.[64] The fluorescence lifetimes for the compounds **1–6** were determined by time correlated single photon counting (TCSPC) and values between 2.8 and 3.7 ns were received, which reflects a shortening of the fluorescence lifetime in respect to pristine 7-hydroxo-cumarine for which a fluorescence lifetime of around 5.7 ns in protic solvents was reported.[65] Taking the observed fluorescence properties of the investigated artemisinin-based hybrid compounds **1–4** and the two reference compounds **5** and **6** into context, all compounds show high quantum yields Φ_{fl} of over 0.75 with **1** exhibiting the highest quantum yield with 0.94. These properties make the compounds highly suitable for fluorescence microscopy-based investigations *in vitro* and flow cytometry analysis.

Table 1 Absorption and emission properties of compounds **1–6** measured in MeOH

	λ_{abs} [a] [nm]	λ_{fl} [b] [nm]	Φ_{fl} [c]	τ_{fl} [ns]
1	348	435	0.94	3.7
2	347	420	0.75	3.2
3	344/399	410	0.75	2.8
4	342/397	409	0.79	3.0
5	348	421	0.89	3.1
6	347	420	0.79	3.1

[a] Long-wavelength absorption maximum. [b] Fluorescence emission maximum; λ_{ex} = 350 nm (λ_{ex} = 320 nm for compound **1**), slit 2/2 nm. [c] Fluorescence quantum yield relative to 9,10-diphenylanthracene in cyclohexane with a fluorescence quantum yield of 0.90.[66]

In vitro antiplasmodial activity of the hybrid drugs

The antiplasmodial activity of artemisinin-coumarin hybrids **1–4** was determined *in vitro* against chloroquine-sensitive 3D7 and chloroquine-/multidrug-resistant Dd2 and K1 parasite strains of *P. falciparum* (Table 2). In general, hybrids **1** and **3** with a non-cleavable ether-based (and shorter) linker between the triazole-coumarin and artemisinin moieties were more potent to inhibit parasite growth compared to their respective hybrid counterparts **2** and **4** with a cleavable ester-linked (and elongated) linker. Moreover, monomeric artemisinin hybrids **1** and **2** were less active than their dimeric artemisinin analogs with comparable linker structure **3**/**4** (Table 2). For the artemisinin-based hybrids **1–4**, IC_{50} values varied from 0.5 nM for **3**, the most potent derivative, to 91.7 nM for **2** when tested against the chloroquine-sensitive strain 3D7. The IC_{50} values decreased for their effect on parasite growth of the chloroquine-/multidrug-resistant strains Dd2 and K1, with K1 always exhibiting the lowest IC_{50} values. Notably, the artemisinin-free coumarin compounds (**5**/**6**) lacked any pronounced antiplasmodial activity, attested by IC_{50} values in the μM range. Both derivates **5**/**6** were slightly more active against the chloroquine-/multidrug-resistant strains (Table 2).

Furthermore, a comparison of the IC_{50} values determined after 24 h *versus* 72 h of drug exposure, presented a comparable plasmodial killing rate for hybrids **1–4** at both incubation times (Table S1 and Fig. S1†). The observed killing rate profile is typical for drugs denoted as fast-acting antimalarials, such as DHA, and starkly contrasts the slow-acting drug atovaquone employed as a threshold, which has a decreased potency to inhibit parasite growth for 24 h *versus* 72 h of drug exposure. Moreover, the presented hybrids achieve rapid parasite growth inhibition without inducing cell toxicity against mammalian cells indicated by high selectivity index (Table 2 and associated Table S1 and Fig. S2†).

In vivo efficacy and stability of the hybrid drugs

The *in vivo* efficacy of hybrid drugs **1–4** was investigated in *P. berghei*-infected mice (Tables 2, S2 and Fig. S3†). While for *in vitro* assays of antimalarial activity, DHA is employed,[68–70] for *in vivo* assays in mice, artesunate (artesunic acid) is used.[71] In line with the *in vitro* studies, the hybrids **1** and **3** with non-cleavable linkers were most efficacious in suppressing parasitemia and thus increasing animal survival. On the contrary, the hybrid **2** with cleavable linker presented, consistent with its relatively low *in vitro* potency, the most inferior efficacy among them. In contrast to its strong *in vitro* potency, cleavable derivative **4** showed a three-fold reduced efficacy than the non-cleavable hybrids **1** and **3**. Overall a clear correlation between the *in*

Table 2 *In vitro* antiplasmodial activity, selectivity index against *P. falciparum* and *in vivo* efficacy in *P. berghei*-infected mice of the hybrid compounds **1–4** and *in vitro* antiplasmodial activity of coumarin derivatives **5/6**

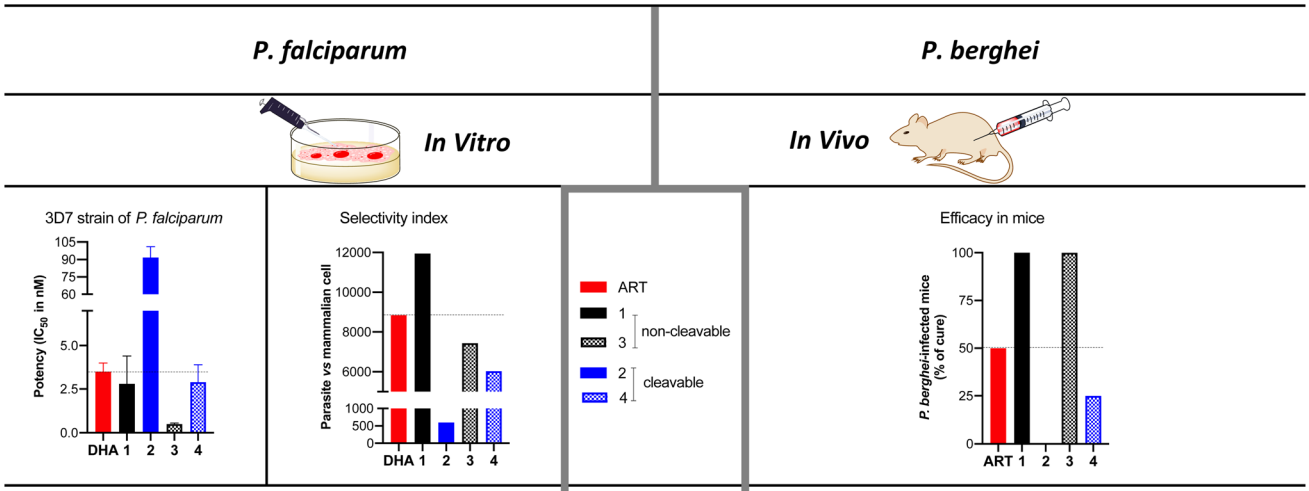

IC_{50} [nM] ± S.E.M.			Selectivity index (SI)	Compound	Dose in mg kg^{-1} (μmol kg^{-1})[c]	Inhibition (% *vs* CTRL)[d]	Median of animal survival in days (cure, %)[e]
3D7[a]	Dd2[a]	K1[a]					
2.8 ± 1.6	2.0 ± 1.3	1.6 ± 0.7	11950	**1**	11.5 (22)	>99	>30[f] (100%)
91.7 ± 9.4	53.4 ± 6.0	40.2 ± 4.2	600	**2**	14 (22)	41.7 ±8.0	18 (0 %)
0.5 ± 0.05	0.5 ± 0.05	0.33 ± 0.04	7442	**3**	18 (22)	>99	>30[f] (100%)
2.9 ± 1.0	2.4 ± 0.4	0.9 ± 0.1	6037	**4**	22 (22)	94 ±11	26 (25 %)
69914.5 ± 4.2	41518.8 ± 3644.2	40710.6 ± 4313.1	N.D.	**5**	N.D.	N.D.	N.D.
118612.6 ± 15421.2	90784.3 ± 6899.2	94822.0 ± 11578.4	N.D.	**6**	N.D.	N.D.	N.D.
3.5 ± 0.5[b]	2.4 ± 0.4[b]	2.4 ± 0.2[b]	8844	**DHA**	N.D.	N.D.	N.D.
14.4 ± 2.0[b]	10.9 ± 0.7[b]	5.2 ± 0.8[b]	N.D.	**Artesunic acid**	8.5 (22)	>99	30[f] (50%)
26.8 ± 2.4[b]	11.3 ± 1.8[b]	5.4 ± 0.5[b]	N.D.	**Artemisinin**	N.D.	N.D.	N.D.
12.7 ± 2.5[b]	165.3 ± 15[b]	302.8 ± 15[b]	N.D.	**Chloroquine**	20 (38)	95 ±10	25 (0%)

[a] *In vitro* inhibitory activity against *P. falciparum* parasites. IC_{50} values are the mean ± S.E.M. (nM) and were determined 72 h after drug exposure. [b] IC_{50} value has been previously reported.[29,67] [c] Treatment was given after 24 h post-infection once-a-day by subcutaneous injection for four consecutive days. [d] Parasitemia inhibition was determined in comparison to vehicle (untreated), determined 48 h after the last day of drug administration and values are mean ± standard deviation. [e] Animal survival was monitored for up to 30 days. Values are from one single experiment, using $n = 5$/group. [f] $p < 0.05$ (Log-rank and Mantel–Cox test) *versus* vehicle.

vitro potency and *in vivo* efficacy of hybrid compounds is observed, as hybrid **3** is the most potent *in vitro* and proved to be the most efficacious *in vivo*.

A dissimilarity in the antimalarial activity among endoperoxide drugs may be related to the stability and degradation of the endoperoxide bridge in red blood cells (RBC). To estimate endoperoxide degradation for the hybrid compounds, we implemented a broadly accepted assay method measuring the parasite-mediated drug degradation[68–70] as outlined in Fig. 2 (panel a). Uninfected RBC (uRBC) were treated with 500 nM of DHA or hybrids **1–4**, supernatants were harvested at indicated times (0.16, 6 and 24 h) and their antimalarial activities were determined against the 3D7 strain of *P. falciparum*. DHA (due to its fast-acting endoperoxide bridge) was employed as a drug susceptible to parasite-mediated degradation, while amodiaquine (AQ) (bearing no endoperoxide unit) was used as a drug not susceptible to heme-mediated reductive degradation.

As depicted in Fig. 2, panel b, the concentration of DHA decreased over time, whereas the concentration of AQ remained unaltered over time. These observations are consistent with previous literature since DHA is a short-living drug rapidly bioactivated and degraded by heme *via* endoperoxide reduction. In contrast, the long-lasting drug AQ is inert to a reductive degradation induced by heme.[68,69] Having set up this, we evaluated the parasite-mediated degradation for hybrid compounds **1–4** (Fig. 2, panel c). As expected, the concentration of the hybrid compounds decreased over time, which is consistent with the notion that any endoperoxide drug is susceptible to parasite-mediated degradation caused by heme. However, as we can infer in Fig. 2, panel d, the drug concentration of all hybrid compounds was higher than DHA. A closer inspection of the equivalent drug concentrations after 24 h revealed that DHA had the lowest concentration among endoperoxide drugs, while compounds **2** and **4** with cleavable linker had the lesser

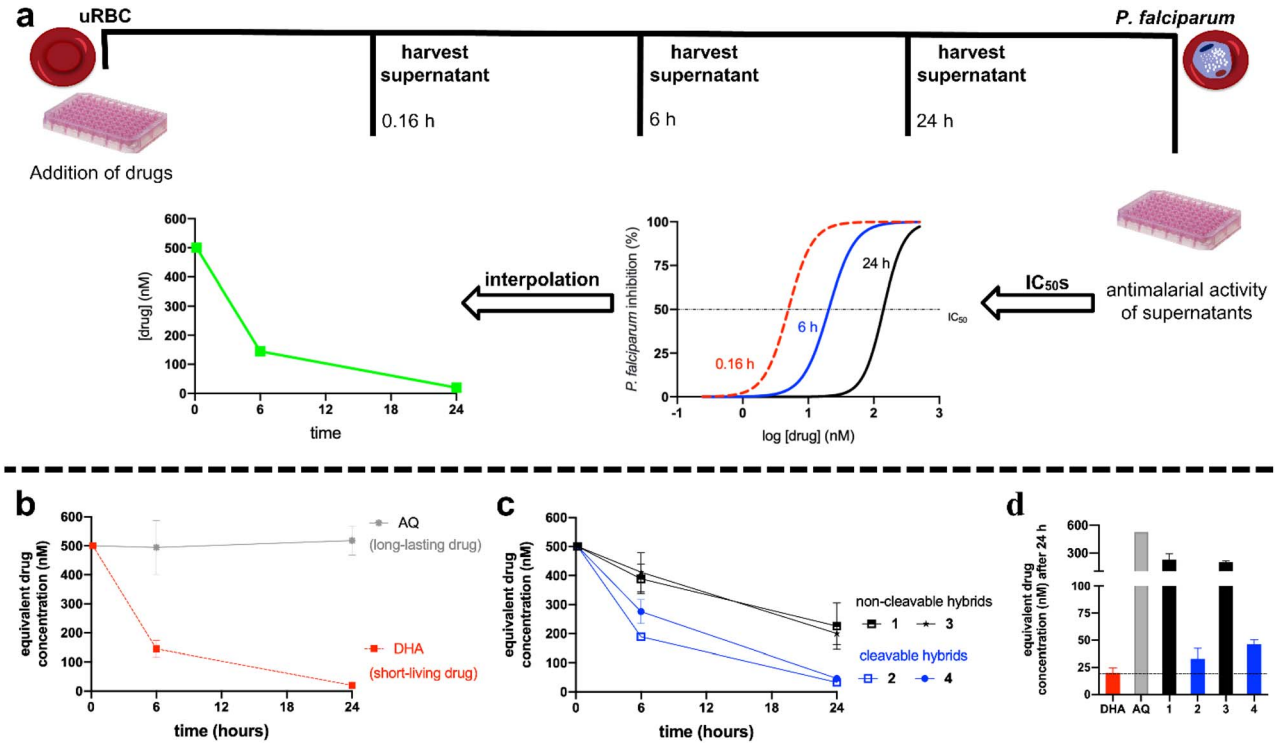

Fig. 2 Panel (a) shows the experimental design for determining the parasite-mediated drug degradation effect. Panel (b) shows the time-dependency concentration for the controls DHA (short-living) and AQ (long-lasting). Panel (c) shows the time-dependency concentration for the hybrids **1**–**4**. Panel (d) compares the drug concentration remaining in the supernatants harvested after 24 h. For panels (b–d): values are the median ± standard error of the mean (S.E.M.) of three independent experiments (each concentration in duplicate). uRBC = uninfected red blood cells; DHA = dihydroartemisinin; AQ = amodiaquine. Full data is disclosed in Table S3.†

concentration among all hybrid compounds. This contrasts with the non-cleavable hybrid compounds **1** and **3**, which had the highest concentration among endoperoxide drugs, albeit their concentrations were lower than for AQ. Of note, while compound **2** with cleavable linker had the lowest *in vitro* potency (Table 2), it was surprisingly less susceptible to reductive degradation of the endoperoxide compared to DHA, which suggests that its low potency is not solely caused by parasite-mediated degradation of its endoperoxide moiety. Its products of degradations are possibly not as potent antimalarial agents as other endoperoxide drugs, such as DHA and artesunate.

Fluorescence imaging in living *P. falciparum*-infected red blood cells

The simplest and readily available hybrid drug **1** with non-cleavable linker, which exhibits an excellent *in vitro* activity (IC_{50} of 2.8 nM in *P. f.* 3D7), high stability, and strong autofluorescence (fluorescence quantum yield of 0.94) was used to assess the localization of the new hybrid compounds in living *P. falciparum*-infected red blood cells. Parasites of the 3D7 strain were incubated with 200 nM of **1** at 37 °C for 0.5, 2, 4, and 8 h, respectively, and costained with the nuclear tracker Syto 13 (see ESI† for detailed information). The fluorescence of **1** was detected using the DAPI filter of an Eclipse Ti microscope for imaging. Uninfected cells were completely unlabeled by **1** (data not shown) under the applied conditions, indicating that accumulation of **1** depends on living parasites. The fluorescence in ring and early trophozoite stages of living parasites was weak and barely detectable. Still, it increased with maturation of the parasite resulting in a peak at the schizont stage.

After short time incubation of 0.5 h and 2 h, hybrid **1** exhibited a diffuse staining pattern in ring, trophozoite and schizont stages (Fig. 3) and did not colocalize with Syto 13 nuclear staining and only rarely and weakly stained the parasite digestive vacuole, visible as an electron dense area within the parasite.

Prolonged incubation periods of 4 h and 8 h, partly resulted in an accumulation of **1** in structures of potentially membranous origin (Fig. 4). However, only younger schizonts and no more mature stages could be observed after prolonged incubation times, indicating that **1** seems to abolish the transition to older schizont stages as these parasites were found to be expelled from their host cells. To investigate a possible localization of hybrid **1** in neutral lipid bodies (NLBs[44]), previously performed with an autofluorescent synthetic endoperoxide as an artemisinin model compound,[72] co-staining with Nile Red (a dye that stains lipids and particularly neutral lipid bodies[73]) was performed (Fig. 4, column E). NLBs are visible as intensely stained spot-like structures adjacent to the food vacuole (Fig. 4, column F, white arrows). In contrast to the rapid accumulation of a fluorescent synthetic endoperoxide in NLBs as described previously,[44] our results do not suggest a colocalization with

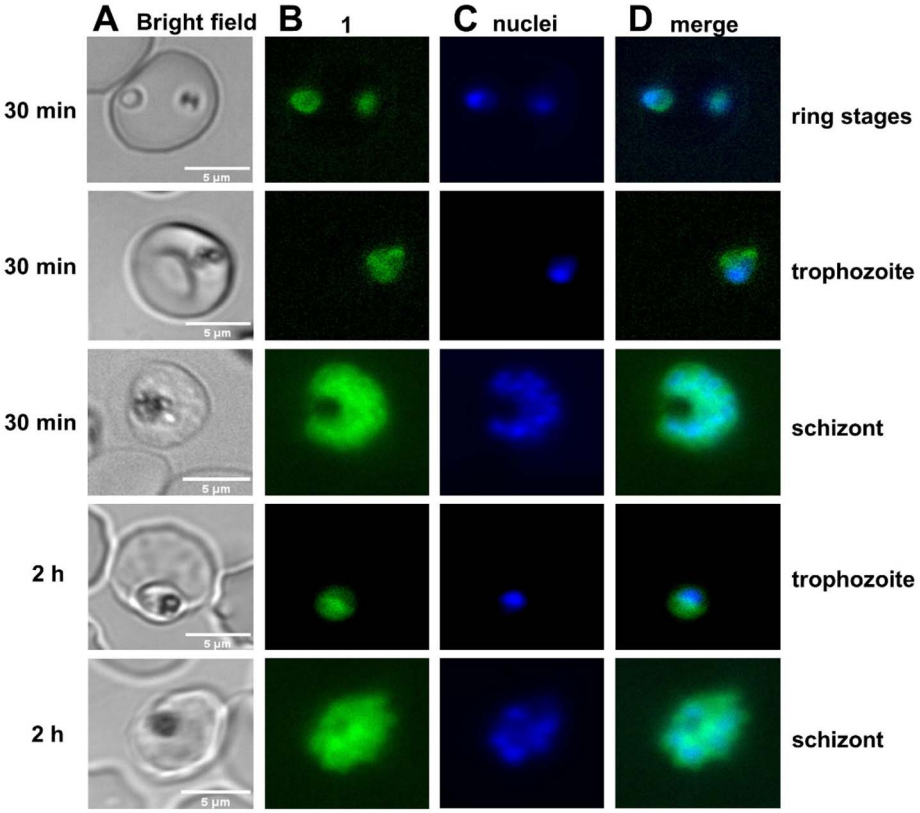

Fig. 3 Bright-field and fluorescence images of ring, trophozoite and schizont stages incubated with **1** for 30 min (rows 1–3) and 2 h (rows 4 and 5) before imaging. Syto 13 staining (blue) indicates the position of nuclei. Column A – bright field image, column B – 1 fluorescence (green), column C – Syto 13 fluorescence (blue); column D – merge of the fluorescence of **1** and Syto 13. White bars represent 5 µm.

NLBs (Fig. 4). Instead, specific Nile Red-stained membranous structures, not identical to NLBs, colocalize with the **1** staining as indicated by the yellow color of the composite. Staining of a similar membranous structure by Nile Red was also previously observed[73] and represents most likely parts of an inner parasitic membrane network. However, compound **1** was also found to stain merozoite membranes (Fig. 4, lane 4).

Although the cellular localization of hybrid **1** in *P. falciparum* was precisely profiled at clinically relevant nanomolar concentrations by microscopy, it remained uncertain if the lipophilicity of the reported hybrids as well as their ability to enter the cells and become bioavailable inside parasites is comparable to DHA. To interrogate this, we profiled the drug uptake of hybrids and DHA in the parasites by flow cytometry and fluorescence in a microplate reader (Fig. S4 and S5† and associated discussion). The estimated concentration of all hybrids **1–4** inside infected RBC (iRBC) was similar to artemisinin-free coumarin compounds **5**/**6** and no significant differences were observed among the hybrids. Moreover, hybrids **1** and **2** were significantly more incorporated by iRBC than uRBC, which depends on drug concentration and the time of drug exposure. Importantly, the uptake of hybrid **1** in iRBC and uRBC was significantly reduced when these cells were previously exposed to DHA. A similar finding was documented in prior literature.[14]

Discussion

Further advances in the combination of high *in vitro*/*in vivo* activity and high intrinsic fluorescence in one hybrid drug will contribute to the progress in the drug discovery due to the possibility of gaining insights into the mode of action of the hybrid drugs. The deliberate design of monomeric and dimeric artemisinin-based coumarin hybrids employing cleavable and non-cleavable linkers enabled a step forward toward the formulation of SAR (structure–activity relationship) and the understanding of the mode of action of artemisinin-based compounds. We demonstrated a straightforward two-step synthetic pathway *via* a key metal-catalyzed click chemistry step to obtain complex artemisinin-coumarin hybrids from commercially available precursors.

The ether-linked artemisinin hybrids **1** and **3** surpass the *in vitro* potency of artemisinin-based drugs DHA, artemisinin and artesunic acid up to 16-fold and exhibit at very least twice the *in vivo* efficacy of artesunate. The same phenotype-based activity is not reproduced by ester linked hybrids **2** and **4**. Interestingly, the studies revealed that the antiplasmodial activity and cytotoxicity of the hybrids in mammalian cells can be clustered according to the chemical structure of the linker. Hybrids containing a non-cleavable ether linker are more potent antiplasmodial agents and more cytotoxic for mammalian cells

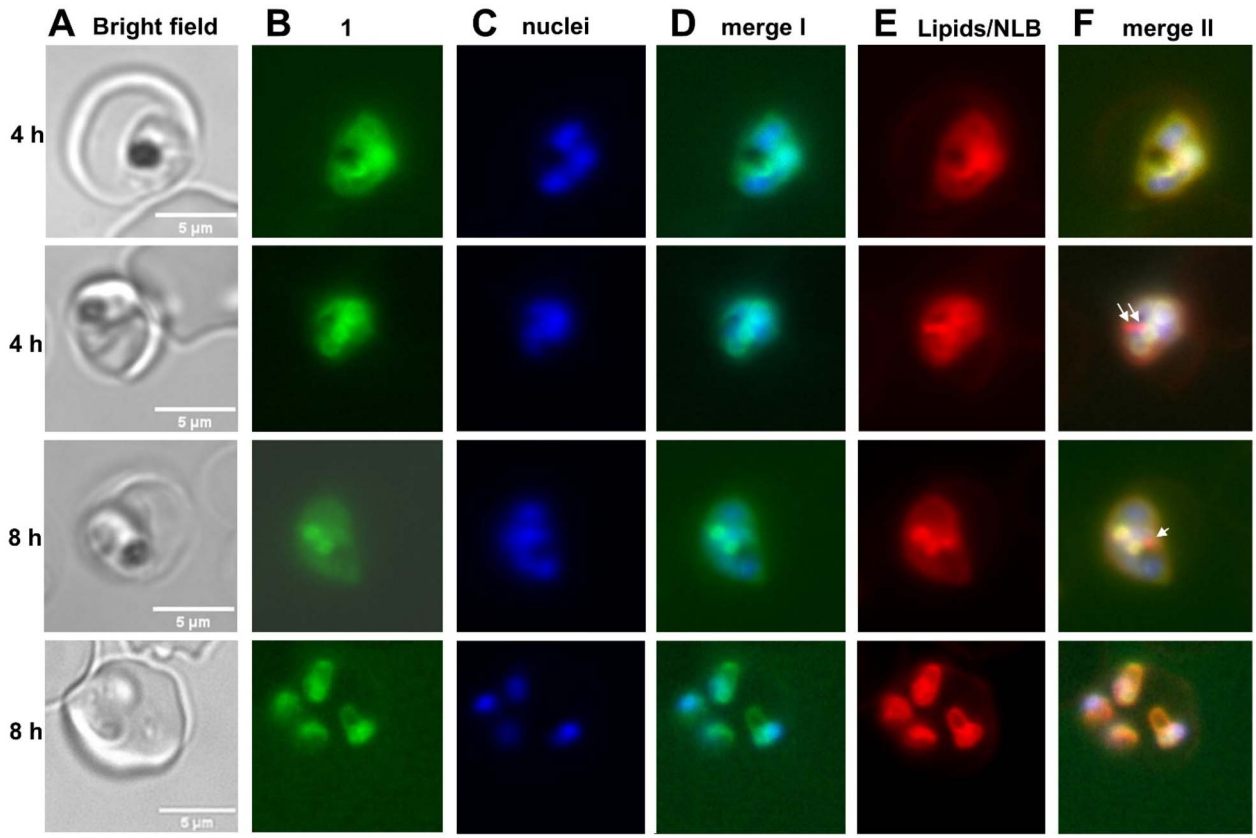

Fig. 4 Bright-field and fluorescence images of schizonts incubated with **1** for 4 h (rows 1 and 2) and 8 h (rows 3 and 4). Syto 13 staining (blue) indicates position of nuclei. Column A – bright field image, column B – **1** fluorescence (green), column C – Syto 13 fluorescence (blue); column D – merge I of the fluorescence of **1** and Syto 13; column E – Nile Red fluorescence: Nile Red stains neutral lipid, in particular neutral lipid bodies; column F – merge II of the fluorescence of **1**, Syto 13 and Nile Red; White bars represent 5 µm. The white arrows indicate the position of NLBs.

than hybrids with a cleavable ester linker. Regarding the importance of one or two endoperoxide units in the composition of hybrids, we concluded from the standard chemosensitivity assays (IC_{50} values) that a hybrid containing two endoperoxide moieties is more potent than a monomeric hybrid of identical linking type. However, a non-cleavable linked hybrid **1** containing only one endoperoxide warhead can equalize (for *P. f.* 3D7) or even surpass (for *P. f.* Dd2) the efficacy of the cleavable linked dimeric hybrid **4**. The most potent monomeric hybrid **1** and dimeric hybrid **3** were less prone to undergo parasite-mediated drug degradation. Multiple analyses shed light on the aspect that an enhancement in potency for endoperoxide drugs is achieved when a long-lasting property (*i.e.*, a stronger chemical stability to resist a heme-mediated degradation than DHA has) is achived.[69,70] This property can be profoundly tuned by the used linker and the effects were found to be pronounced for hybrids carrying two endoperoxide units in the reported library. Our SAR model dictates that if two endoperoxide moieties are combined using a non-cleavable chemical linker, as for the hybrid **3**, a strong and efficacious antimalarial drug with a 10-fold increase in stability and a 7-fold increase in activity compared to DHA is observed.

As previously mentioned, the high intrinsic fluorescence of hybrid **1** ($\Phi_{fl} = 0.94$, Table 1) combined with its high *in vitro* and *in vivo* potency and efficacy made it most suitable for live-cell imaging, which enabled a precise profiling of the cellular localization of **1** in living *P. falciparum* parasites by fluorescence microscopy at low nanomolar drug concentrations, reproducing the therapy in humans. The timing of **1**-staining and co-staining procedures both revealed a diffusion of **1** over the cytoplasm of parasite cells for short incubation times (0.5 h to 2 h). Even after prolonged incubation times (4 h to 8 h), **1** was not preferentially localized inside the parasite's digestive vacuole, consistent with a precedent report.[14] Moreover, we found membranous structures stained by **1** in both mature parasite stages and merozoites. In contrast, previously a synthetic fluorescent artemisinin model compound was found to accumulate in neutral lipid bodies (NLB) at micromolar concentrations.[44]

As hybrids possess chemical functionalization, this may lead to alterations in their uptake and cellular localization in comparison to artemisinins used in patients, like DHA and artesunate. We found that all compounds **1–6** can become bioavailable for uptake in RBC, as expected to occur in any small molecule able to cross lipid membranes by passive permeability. However, hybrids **1–4** were preferentially accumulated in parasites than host cells. This is consistent with the visualization of hybrid **1** inspected by microscopy. Moreover, we found that the uptake of hybrid **1** in RBC was mitigated in the presence of DHA. Meanwhile, this is not surprising, given that both are endoperoxides derived from the same 1,2,4-trioxane ring and no

alteration in the trioxane ring was performed to design hybrids, this supports the reliable and robustness of autofluorescent hybrids for studying artemisinin's cellular localization. Based on these findings, we argue that the cellular localization of **1** likely reflects the artemisinins used in patients. Finally, our data indicates that a stronger potency and efficacy for hybrid **1** *versus* DHA/artesunate is achieved because of its stability to overcome parasite-mediated drug degradation. These data justify further studies in artemisinin-resistant parasites in the future.

Conclusions

We have designed and synthesized first autofluorescent antimalarial artemisinin-coumarin hybrids **1–4**, which combine two desired features in one drug compound: high *in vitro*/*in vivo* activity and high intrinsic fluorescence suitable for live-cell imaging. These new hybrids, with non-cleavable (ether) and cleavable (ester) linkers and featuring one or two endoperoxide moieties were obtained *via* metal-catalyzed click chemistry from readily available alkyne and azide precursors. The hybrids exhibit excellent antimalarial activity *in vitro* against CQ-resistant and multidrug-resistant *P. falciparum* strains (IC_{50}(Dd2) down to 0.5 nM; IC_{50}(K1) down to 0.33 nM) compared to reference drugs CQ (IC_{50}(Dd2) = 165.3 nM; IC_{50}(K1) = 302.8 nM) and artemisinin (IC_{50}(Dd2) = 11.3 nM; IC_{50}(K1) = 5.4 nM). A combination of photophysical analysis, microscopy, and flow cytometry have revealed the high suitability of hybrids for real-time imaging in living parasite cells at clinically relevant low drug concentration when the parasite-mediated degradation of artemisinins is circumvented. Furthermore, it was found that hybrids featuring two endoperoxide units have improved *in vitro*/*in vivo* antimalarial activities compared to hybrids with only one endoperoxide moiety. Notably, a metabolically resistant non-cleavable chemical linker should be employed (*e.g.*, hybrid compound **3**) to achieve the best potency. In general, our findings should provide a valuable basis for autofluorescent artemisinin-based antimalarial drug design suitable for cellular uptake visualization and fluorescence imaging in living *P. falciparum*-infected red blood cells. Our results should also encourage further mechanistic studies and be a stepping stone toward overcoming multidrug resistance.

Ethical statement

Experiments were conducted in 2019–2022 in accordance with the recommendations of ethical issues guidelines and were approved (protocol 020/2018) by the local Animal Ethics Committee at Fiocruz Bahia (IGM,Salvador, Brazil).

Data availability

All data are available from the authors upon reasonable request.

Author contributions

L. H., C. M. and A. Ç. carried out all synthetic work and conducted the click reactions. M. L. performed the *in vitro* and live-cell imaging studies under the supervision of B. K., A. S. M. and M. C. B. S. performed the *in vivo* studies under the supervision of D. R. M. M., F. P. and A. K. carried out the photophysical measurements. D. R. M. M., B. K. and S. B. T. designed and supervised the experimental outline of the corresponding studies. L. H., D. R. M. M., B. K., S. B. T. wrote the manuscript with input from all authors. S. B. T. conceived and directed the research.

Conflicts of interest

There are no conflicts to declare.

Acknowledgements

S. B. T. gratefully acknowledges the financial support from the Deutsche Forschungsgemeinschaft (DFG, Grant TS 87/23-1) and the Volkswagen Foundation (Project: Innovative Approaches to Drug Development). D. R. M. M. acknowledges CNPq (Brazil, grant 440227/2022-4) and Fapesb (Brazil, grant PIE0009/2022).

References

1 D. J. Newman and G. M. Cragg, Natural Products as Sources of New Drugs from 1981 to 2014, *J. Nat. Prod.*, 2016, **79**, 629–661.
2 X.-Z. Su and L. H. Miller, The discovery of artemisinin and the Nobel Prize in Physiology or Medicine, *Sci. China: Life Sci.*, 2015, **58**, 1175–1179.
3 Y. Tu, Artemisinin—A Gift from Traditional Chinese Medicine to the World (Nobel Lecture), *Angew. Chem., Int. Ed.*, 2016, **55**, 10210–10226.
4 T. Efferth, H. Dunstan, A. Sauerbrey, H. Miyachi and C. R. Chitambar, The anti-malarial artesunate is also active against cancer, *Int. J. Oncol.*, 2001, **18**, 767–773.
5 R. D. Slack, A. M. Jacobine and G. H. Posner, Antimalarial peroxides: advances in drug discovery and design, *MedChemComm*, 2012, **3**, 281–297.
6 J. Wang, J. Zhang, Y. Shi, C. Xu, C. Zhang, Y. K. Wong, Y. M. Lee, S. Krishna, Y. He, T. K. Lim, W. Sim, Z. C. Hua, H. M. Shen and Q. Lin, Mechanistic Investigation of the Specific Anticancer Property of Artemisinin and Its Combination with Aminolevulinic Acid for Enhanced Anticolorectal Cancer Activity, *ACS Cent. Sci.*, 2017, **3**, 743–750.
7 Y. K. Wong, C. Xu, K. A. Kalesh, Y. He, Q. Lin, W. S. F. Wong, H.-M. Shen and J. Wang, Artemisinin as an anticancer drug: Recent advances in target profiling and mechanisms of action, *Med. Res. Rev.*, 2017, **37**, 1492–1517.
8 T. Fröhlich, F. Hahn, L. Belmudes, M. Leidenberger, O. Friedrich, B. Kappes, Y. Couté, M. Marschall and S. B. Tsogoeva, Synthesis of Artemisinin-Derived Dimers, Trimers and Dendrimers: Investigation of Their Antimalarial and Antiviral Activities Including Putative Mechanisms of Action, *Chem.–Eur. J.*, 2018, **24**, 8103–8113.
9 B. Golankiewicz, T. Ostrowski, T. Goslinski, P. Januszczyk, J. Zeidler, D. Baranowski and E. de Clercq, Fluorescent

Tricyclic Analogues of Acyclovir and Ganciclovir. A Structure−Antiviral Activity Study, *J. Med. Chem.*, 2001, **44**, 4284–4287.

10 J. Broichhagen and N. Kilian, Chemical Biology Tools To Investigate Malaria Parasites, *ChemBioChem*, 2021, **22**, 2219–2236.

11 J. B. Grimm and L. D. Lavis, Caveat fluorophore: an insiders' guide to small-molecule fluorescent labels, *Nat. Methods*, 2022, **19**, 149–158.

12 T. Terai and T. Nagano, Small-molecule fluorophores and fluorescent probes for bioimaging, *Pflug. Arch. Eur. J. Physiol.*, 2013, **465**, 347–359.

13 J. Wang, C. J. Zhang, W. N. Chia, C. C. Loh, Z. Li, Y. M. Lee, Y. He, L. X. Yuan, T. K. Lim, M. Liu, C. X. Liew, Y. Q. Lee, J. Zhang, N. Lu, C. T. Lim, Z. C. Hua, B. Liu, H. M. Shen, K. S. Tan and Q. Lin, Haem-activated promiscuous targeting of artemisinin in Plasmodium falciparum, *Nat. Commun.*, 2015, **6**, 10111–10122.

14 A. Sissoko, P. Vásquez-Ocmín, A. Maciuk, D. Barbieri, G. Neveu, L. Rondepierre, R. Grougnet, P. Leproux, M. Blaud, K. Hammad, S. Michel, C. Lavazec, J. Clain, S. Houzé and R. Duval, A Chemically Stable Fluorescent Mimic of Dihydroartemisinin, Artemether, and Arteether with Conserved Bioactivity and Specificity Shows High Pharmacological Relevance to the Antimalarial Drugs, *ACS Infect. Dis.*, 2020, **6**, 1532–1547.

15 H. M. Ismail, V. E. Barton, M. Panchana, S. Charoensutthivarakul, G. A. Biagini, S. A. Ward and P. M. O'Neill, A Click Chemistry-Based Proteomic Approach Reveals that 1,2,4-Trioxolane and Artemisinin Antimalarials Share a Common Protein Alkylation Profile, *Angew. Chem., Int. Ed.*, 2016, **55**, 6401–6405.

16 U. Eckstein-Ludwig, R. J. Webb, I. D. A. van Goethem, J. M. East, A. G. Lee, M. Kimura, P. M. O'Neill, P. G. Bray, S. A. Ward and S. Krishna, Artemisinins target the SERCA of Plasmodium falciparum, *Nature*, 2003, **424**, 957–961.

17 F. E. Held, A. A. Guryev, T. Fröhlich, F. Hampel, A. Kahnt, C. Hutterer, M. Steingruber, H. Bahsi, C. von Bojničić-Kninski, D. S. Mattes, T. C. Foertsch, A. Nesterov-Mueller, M. Marschall and S. B. Tsogoeva, Facile access to potent antiviral quinazoline heterocycles with fluorescence properties via merging metal-free domino reactions, *Nat. Commun.*, 2017, **8**, 15071–15080.

18 M. M. Lee, Z. Gao and B. R. Peterson, Synthesis of a Fluorescent Analogue of Paclitaxel That Selectively Binds Microtubules and Sensitively Detects Efflux by P-Glycoprotein, *Angew. Chem., Int. Ed.*, 2017, **56**, 6927–6931.

19 L. Herrmann, F. Hahn, B. W. Grau, M. Wild, A. Niesar, C. Wangen, E. Kataev, M. Marschall and S. B. Tsogoeva, Autofluorescent Artemisinin-Benzimidazole Hybrids via Organo-Click Reaction: Study of Antiviral Properties and Mode of Action in Live Cells, *Chem. - Eur. J.*, 2023, e202301194.

20 L. F. Tietze, H. P. Bell and S. Chandrasekhar, Natural Product Hybrids as New Leads for Drug Discovery, *Angew. Chem., Int. Ed.*, 2003, **42**, 3996–4028.

21 S. B. Tsogoeva, Recent Progress in the Development of Synthetic Hybrids of Natural or Unnatural Bioactive Compounds for Medicinal Chemistry, *Mini-Rev. Med. Chem.*, 2010, **10**, 773–793.

22 B. Sharma, P. Singh, A. K. Singh and S. K. Awasthi, Advancement of chimeric hybrid drugs to cure malaria infection: An overview with special emphasis on endoperoxide pharmacophores, *Eur. J. Med. Chem.*, 2021, **219**, 113408–113444.

23 H. M. Sampath Kumar, L. Herrmann and S. B. Tsogoeva, Structural hybridization as a facile approach to new drug candidates, *Bioorg. Med. Chem. Lett.*, 2020, **30**, 127514–127528.

24 G. Mehta and V. Singh, Hybrid systems through natural product leads: An approach towards new molecular entities, *Chem. Soc. Rev.*, 2002, **31**, 324–334.

25 J. J. Walsh, D. Coughlan, N. Heneghan, C. Gaynor and A. Bell, A novel artemisinin-quinine hybrid with potent antimalarial activity, *Bioorg. Med. Chem.*, 2007, **17**, 3599–3602.

26 N. Wang, K. J. Wicht, E. Shaban, T. A. Ngoc, M. Q. Wang, I. Hayashi, M. I. Hossain, Y. Takemasa, M. Kaiser, I. E. El Sayed, T. J. Egan and T. Inokuchi, Synthesis and evaluation of artesunate-indoloquinoline hybrids as antimalarial drug candidates, *MedChemComm*, 2014, **5**, 927–931.

27 T. Fröhlich, C. Reiter, M. M. Ibrahim, J. Beutel, C. Hutterer, I. Zeitträger, H. Bahsi, M. Leidenberger, O. Friedrich, B. Kappes, T. Efferth, M. Marschall and S. B. Tsogoeva, Synthesis of Novel Hybrids of Quinazoline and Artemisinin with High Activities against Plasmodium falciparum, Human Cytomegalovirus, and Leukemia Cells, *ACS Omega*, 2017, **2**, 2422–2431.

28 T. Frohlich, C. Reiter, M. E. M. Saeed, C. Hutterer, F. Hahn, M. Leidenberger, O. Friedrich, B. Kappes, M. Marschall, T. Efferth and S. B. Tsogoeva, Synthesis of Thymoquinone-Artemisinin Hybrids: New Potent Antileukemia, Antiviral, and Antimalarial Agents, *ACS Med. Chem. Lett.*, 2018, **9**, 534–539.

29 A. Çapcı, M. Lorion, H. Wang, N. Simon, M. Leidenberger, M. Borges Silva, D. Moreira, Y. Zhu, Y. Meng, J. Y. Chen, Y. Lee, O. Friedrich, B. Kappes, J. Wang, L. Ackermann and S. B. Tsogoeva, Artemisinin-(Iso)quinoline Hybrids by C-H Activation and Click Chemistry: Combating Multidrug-Resistant Malaria, *Angew. Chem., Int. Ed.*, 2019, **58**, 13066–13079.

30 H. Yu, Z. Hou, Y. Tian, Y. Mou and C. Guo, Design, synthesis, cytotoxicity and mechanism of novel dihydroartemisinin-coumarin hybrids as potential anti-cancer agents, *Eur. J. Med. Chem.*, 2018, **151**, 434–449.

31 C. Zippilli, S. Filippi, S. Cesarini, B. M. Bizzarri, P. Conigliaro, E. De Marchi, L. Botta and R. Saladino, Synthesis of Artesunic Acid–Coumarin Hybrids as Potential Antimelanoma Agents, *ACS Med. Chem. Lett.*, 2023, **14**, 599–605.

32 Y. Tian, Z. Liang, H. Xu, Y. Mou and C. Guo, Design, Synthesis and Cytotoxicity of Novel Dihydroartemisinin-

Coumarin Hybrids via Click Chemistry, *Molecules*, 2016, **21**, 758.

33 E.-J. Seo, M. Saeed, B. Y. Law, A. G. Wu, O. Kadioglu, H. J. Greten and T. Efferth, Pharmacogenomics of Scopoletin in Tumor Cells, *Molecules*, 2016, **21**, 496–518.

34 P. J. Weathers, M. Towler, A. Hassanali, P. Lutgen and P. O. Engeu, Dried-leaf Artemisia annua: A practical malaria therapeutic for developing countries?, *World J. Pharmacol.*, 2014, **3**, 39–55.

35 A. Malik, A. Kushnoor, V. Saini, S. Singhal, S. Kumar and Y. C. Yadav, In vitro antioxidant properties of Scopoletin, *J. Chem. Pharm. Res.*, 2011, **3**, 659–665.

36 K.-M. Li, X. Dong, Y.-N. Ma, Z.-H. Wu, Y.-M. Yan and Y.-X. Cheng, Antifungal coumarins and lignans from Artemisia annua, *Fitoterapia*, 2019, **134**, 323–328.

37 D. L. Klayman, Artemisinin: an Antimalarial Drug from China, *Science*, 1985, **228**, 1049–1055.

38 G. J. B. Gnonlonfin, A. Sanni and L. Brimer, Review Scopoletin – A Coumarin Phytoalexin with Medicinal Properties, *Crit. Rev. Plant Sci.*, 2012, **31**, 47–56.

39 M. Lončarić, D. Gašo-Sokač, S. Jokić and M. Molnar, Recent Advances in the Synthesis of Coumarin Derivatives from Different Starting Materials, *Biomolecules*, 2020, **10**, 151.

40 R. H. Vekariya and H. D. Patel, Recent Advances in the Synthesis of Coumarin Derivatives via Knoevenagel Condensation: A Review, *Synth. Commun.*, 2014, **44**, 2756–2788.

41 A. Bouhaoui, M. Eddahmi, M. Dib, M. Khouili, A. Aires, M. Catto and L. Bouissane, Synthesis and Biological Properties of Coumarin Derivatives. A Review, *ChemistrySelect*, 2021, **6**, 5848–5870.

42 J. A. Key, S. Koh, Q. K. Timerghazin, A. Brown and C. W. Cairo, Photophysical characterization of triazole-substituted coumarin fluorophores, *Dyes Pigm.*, 2009, **82**, 196–203.

43 K. Sivakumar, F. Xie, B. M. Cash, S. Long, H. N. Barnhill and Q. Wang, A Fluorogenic 1,3-Dipolar Cycloaddition Reaction of 3-Azidocoumarins and Acetylenes, *Org. Lett.*, 2004, **6**, 4603–4606.

44 C. L. Hartwig, A. S. Rosenthal, J. D'Angelo, C. E. Griffin, G. H. Posner and R. A. Cooper, Accumulation of artemisinin trioxane derivatives within neutral lipids of Plasmodium falciparum malaria parasites is endoperoxide-dependent, *Biochem. Pharmacol.*, 2009, **77**, 322–336.

45 H. C. Kolb, M. G. Finn and K. B. Sharpless, Click Chemistry: Diverse Chemical Function from a Few Good Reactions, *Angew. Chem., Int. Ed.*, 2001, **40**, 2004–2021.

46 L. Zhang, X. Chen, P. Xue, H. H. Y. Sun, I. D. Williams, K. B. Sharpless, V. V. Fokin and G. Jia, Ruthenium-Catalyzed Cycloaddition of Alkynes and Organic Azides, *J. Am. Chem. Soc.*, 2005, **127**, 15998–15999.

47 C. R. Harding, S. M. Sidik, B. Petrova, N. F. Gnädig, J. Okombo, A. L. Herneisen, K. E. Ward, B. M. Markus, E. A. Boydston, D. A. Fidock and S. Lourido, Genetic screens reveal a central role for heme metabolism in artemisinin susceptibility, *Nat. Commun.*, 2020, **11**, 4813–4830.

48 L. E. Heller, E. Goggins and P. D. Roepe, Dihydroartemisinin–Ferriprotoporphyrin IX Adduct Abundance in Plasmodium falciparum Malarial Parasites and the Relationship to Emerging Artemisinin Resistance, *Biochemistry*, 2018, **57**, 6935–6945.

49 B. R. Blank, R. L. Gonciarz, P. Talukder, J. Gut, J. Legac, P. J. Rosenthal and A. R. Renslo, Antimalarial Trioxolanes with Superior Drug-Like Properties and In Vivo Efficacy, *ACS Infect. Dis.*, 2020, **6**, 1827–1835.

50 F. Bousejra-El Garah, M. H.-L. Wong, R. K. Amewu, S. Muangnoicharoen, J. L. Maggs, J.-L. Stigliani, B. K. Park, J. Chadwick, S. A. Ward and P. M. O'Neill, Comparison of the Reactivity of Antimalarial 1,2,4,5-Tetraoxanes with 1,2,4-Trioxolanes in the Presence of Ferrous Iron Salts, Heme, and Ferrous Iron Salts/Phosphatidylcholine, *J. Med. Chem.*, 2011, **54**, 6443–6455.

51 A. Çapcı, L. Herrmann, H. M. Sampath Kumar, T. Fröhlich and S. B. Tsogoeva, Artemisinin-derived dimers from a chemical perspective, *Med. Res. Rev.*, 2021, **41**, 2927–2970.

52 B. Zhang, Artemisinin-derived dimers as potential anticancer agents: Current developments, action mechanisms, and structure–activity relationships, *Arch. Pharm.*, 2020, **353**, 1900240–19000251.

53 V. Tuan Kien, L. Huy Binh, P. Hai Phong, D. Thi Hien, N. Thi Thuy My, N. Hai Nam, D. Thi Thao, M. Baltas and T. Khac Vua, Novel Artemisinin-Derived Dimers: Synthesis and Evaluation of Anti-cancer Activities, *Lett. Drug Des. Discovery*, 2017, **14**, 102–111.

54 A. N. Pearce, M. Kaiser and B. R. Copp, Synthesis and antimalarial evaluation of artesunate-polyamine and trioxolane-polyamine conjugates, *Eur. J. Med. Chem.*, 2017, **140**, 595–603.

55 T. Fröhlich, A. Çapcı, C. Reiter and S. B. Tsogoeva, Artemisinin-Derived Dimers: Potent Antimalarial and Anticancer Agents, *J. Med. Chem.*, 2016, **59**, 7360–7388.

56 P. P. Bora, N. Baruah, G. Bez and N. C. Barua, New Method for the Synthesis of Ether Derivatives of Artemisinin, *Synth. Commun.*, 2012, **42**, 1218–1225.

57 A. Brossi, B. Venugopalan, L. Dominguez Gerpe, H. J. C. Yeh, J. L. Flippen-Anderson, P. Buchs, X. D. Luo, W. Milhous and W. Peters, Arteether, a new antimalarial drug: synthesis and antimalarial properties, *J. Med. Chem.*, 1988, **31**, 645–650.

58 A. Çapcı, C. Reiter, E. J. Seo, L. Gruber, F. Hahn, M. Leidenberger, V. Klein, F. Hampel, O. Friedrich, M. Marschall, B. Kappes, T. Efferth and S. B. Tsogoeva, Access to new highly potent antileukemia, antiviral and antimalarial agents via hybridization of natural products (homo)egonol, thymoquinone and artemisinin, *Bioorg. Med. Chem.*, 2018, **26**, 3610–3618.

59 J. R. Heldt, J. Heldt, M. Stoń and H. A. Diehl, Photophysical properties of 4-alkyl- and 7-alkoxycoumarin derivatives. Absorption and emission spectra, fluorescence quantum yield and decay time, *Spectrochim. Acta, Part A*, 1995, **51**, 1549–1563.

60 M. Chatterjee, S. Chatterjee, M. Basu Roy, S. Ghosh, P. Bandyopadhyay and P. K. Bharadwaj, Photophysical

properties of tris-methoxycoumarin derivative of a cryptand, *J. Lumin.*, 2002, **99**, 175–183.

61 W.-C. Sun, K. R. Gee and R. P. Haugland, Synthesis of novel fluorinated coumarins: Excellent UV-light excitable fluorescent dyes, *Bioorg. Med. Chem. Lett.*, 1998, **8**, 3107–3110.

62 K. Sen and P. Bagchi, Studies on the Ultraviolet Absorption Spectra of Coumarins and Chromones. II. Hydroxy Derivatives1, *J. Org. Chem.*, 1959, **24**, 316–319.

63 M. Hoshiyama, K. Kubo, T. Igarashi and T. Sakurai, Complexation and proton dissociation behavior of 7-hydroxy-4-methylcoumarin and related compounds in the presence of β-cyclodextrin, *J. Photochem. Photobiol., A*, 2001, **138**, 227–233.

64 J. E. Fortier, P. Even-Hernandez, F. Baros, S. Poulain, N. Martinet, M. Donner, C. Gouyette and M. C. Carré, The synthesis, photophysical properties and energy transfer of a coumarin-based bichromophoric compound, *Dyes Pigm.*, 2009, **80**, 115–120.

65 T. Moriya, Excited-state Reactions of Coumarins in Aqueous Solutions. I. The Phototautomerization of 7-Hydroxycoumarin and Its Derivative, *Bull. Chem. Soc. Jpn.*, 1983, **56**, 6–14.

66 S. Hamai and F. Hirayama, Actinometric determination of absolute fluorescence quantum yields, *J. Phys. Chem.*, 1983, **87**, 83–89.

67 H. C. Quadros, A. Çapcı, L. Herrmann, S. D'Alessandro, D. Fontinha, R. Azevedo, W. Villarreal, N. Basilico, M. Prudêncio, S. B. Tsogoeva and D. R. M. Moreira, Studies of Potency and Efficacy of an Optimized Artemisinin-Quinoline Hybrid against Multiple Stages of the Plasmodium Life Cycle, *Pharmaceuticals*, 2021, **14**, 1129–1146.

68 Y. Du, C. Giannangelo, W. He, J. Shami Gerald, W. Zhou, T. Yang, J. Creek Darren, C. Dogovski, X. Li and L. Tilley, Dimeric Artesunate Glycerophosphocholine Conjugate Nano-Assemblies as Slow-Release Antimalarials to Overcome Kelch 13 Mutant Artemisinin Resistance, *Antimicrob. Agents Chemother.*, 2022, **66**, e02065-21.

69 T. Yang, C. Xie Stanley, P. Cao, C. Giannangelo, J. McCaw, J. Creek Darren, A. Charman Susan, N. Klonis and L. Tilley, Comparison of the Exposure Time Dependence of the Activities of Synthetic Ozonide Antimalarials and Dihydroartemisinin against K13 Wild-Type and Mutant Plasmodium falciparum Strains, *Antimicrob. Agents Chemother.*, 2016, **60**, 4501–4510.

70 C. Giannangelo, L. Stingelin, T. Yang, L. Tilley, A. Charman Susan and J. Creek Darren, Parasite-Mediated Degradation of Synthetic Ozonide Antimalarials Impacts In Vitro Antimalarial Activity, *Antimicrob. Agents Chemother.*, 2018, **62**, e01566-17.

71 F. R. Radohery Georges, A. Walz, C. Gumpp, H. Cherkaoui-Rbati Mohammed, N. Gobeau, J. Gower, P. Davenport Miles, M. Rottmann, S. McCarthy James, J. Möhrle Jörg, M. Rebelo, C. Demarta-Gatsi and S. Khoury David, Parasite Viability as a Measure of In Vivo Drug Activity in Preclinical and Early Clinical Antimalarial Drug Assessment, *Antimicrob. Agents Chemother.*, 2022, **66**, e00114–e00122.

72 G. H. Posner, C. H. Oh, L. Gerena and W. K. Milhous, Extraordinarily potent antimalarial compounds: new, structurally simple, easily synthesized, tricyclic 1,2,4-trioxanes, *J. Med. Chem.*, 1992, **35**, 2459–2467.

73 K. E. Jackson, N. Klonis, D. J. P. Ferguson, A. Adisa, C. Dogovski and L. Tilley, Food vacuole-associated lipid bodies and heterogeneous lipid environments in the malaria parasite, Plasmodium falciparum, *Mol. Microbiol.*, 2004, **54**, 109–122.